J Appl Math Comput (2008) 28: 235–247
DOI 10.1007/s12190-008-0097-5

JAMC

Laminar flow separation in an axi-symmetric sudden smooth expanded circular tube

G.C. Layek · S. Mukhopadhyay

Received: 26 April 2007 / Revised: 30 August 2007 / Published online: 20 June 2008

Abstract This paper concerns with the investigation of laminar flow separation and its consequences in a tube over a smooth expansion under the axi-symmetric approximations. A co-ordinate stretching has been made to map the expanded tube into a straight tube. The two-dimensional unsteady Navier-Stokes equations are solved approximately by using primitive variables in staggered grid. A thorough quantitative analysis is performed through numerical simulations of the desired quantities such as wall shear stress, axial velocity, pressure distribution etc. These quantities are presented graphically and their consequences in the flow field are analysed in details. The dependence of the flow field on the physical parameter like expansion height d and on the Reynolds number has been investigated in details. It is interesting to note that the peak value of wall shear stress decreases with increasing height of expansion and also with the increasing Reynolds number.

Keywords Axi-symmetric flow · Laminar flow · Smooth expansion · Finite difference scheme

Mathematics Subject Classification (2000) 76XX · 76DXX · 92C10

1 Introduction

The analysis of steady as well as unsteady flow in close conduits is a topic relevant to many different fields like engineering and biomechanics, in particular, human

G.C. Layek (✉)
Department of Mathematics, The University of Burdwan, Burdwan 713104, W.B., India
e-mail: math_gclayek@buruniv.ac.in

S. Mukhopadhyay
Department of Mathematics, M.U.C. Women's College, Burdwan 713104, W.B., India
e-mail: swati_bumath@yahoo.co.in

cardio-vascular system. Inspite of practical interest, such type of flow can lead to complex phenomena, even in simple external conditions having intrinsic theoretical importance.

Flows through sudden expansions are frequently encountered in many industries, and therefore, are of strong interest from practical point of view. The study of laminar flow over expansion has developed significantly in the last decade. The greater part of these analysis deals with sudden expansions in the form of a step but the global behaviour does not differ drastically from this until a smooth expansion is able to produce a significant separated flow. Although the flow is complex, typically exhibiting three distinct regions-separation, recirculation and reattachment-the fact that the separation point is fixed at the edge of the sudden expansion simplifies the analysis of the flow. Furthermore, the axi-symmetric flow geometry affords a straight forward numerical implementation in cylindrical coordinates (Hammad et al. [5]).

Vascular fluid dynamics plays an important role in the development and progression of arterial diseases like stenosis, aneurysm. It is very difficult to measure blood flow, particularly that within the human body, with sufficient precision in order to determine the local influence of fluid mechanical factors with respect to physiological and pathological phenomena. Recently, several numerical studies (Taylor et al. [12], Formaggia et al. [2], Yamaguchi [13]) have been carried out to trace the hemodynamics in blood vessels. Study of steady and unsteady flow dynamics in vessels with either constrictions or dilations is of paramount importance in understanding the influence of arterial diseases on regional blood flow and in the design of artificial organs like oxygenerator. Specially the analysis of flow in vessels with dilation can help in understanding the influence of hemodynamic factors like wall shear stress (WSS), wall pressure (WP), velocities on the growth of arterial diseases.

The present work deals with the steady laminar flow inside a circular tube with a smooth expansion. The wall of arterial segment is considered to be rigid. When stenoses or aneurysms develop in human vasculature, the vessel walls in the vicinity of the stenosis or aneurysm are usually relatively solid. Detailed description of the flow field, in terms of incompressible fluid dynamics over rigid walls, can help the search for an explanation of the post-surgical complications occurring in some carotid operations. The use of the linearized Navier-Stokes equations may suit well for explaining some aspects of hemodynamic flow in smaller arteries, but for larger arteries, consideration of the nonlinear terms in the Navier-Stokes equations governing the flow of blood becomes indispensable. For two-dimensional flow in larger arteries they are of major significance having large dynamic storage effects (Ling and Atabek [8]). Keeping this motivation in mind, the investigation is carried out by the numerical simulation of the unsteady nonlinear Navier-Stokes equations in the axi-symmetric approximation. Finite-difference staggered grid is employed to solve the governing equations of the fluid flow. A co-ordinate transformation is employed to map a long irregular geometry into a straight circular tube. A detailed investigation is done to realise the flow dependence on the expansion value (height d) and the Reynolds number. Further, instantaneous velocity and pressure fields would help in analyzing the subtle features associated with flow field like the development of recirculation regions, vortex formation etc.

2 Equations of motion

We consider an axi-symmetric and laminar separated flow in a smooth expanded tube, expanded at the specified position. Let (r^*, θ^*, z^*) be the cylindrical polar coordinates with z^*-axis along the axis of symmetry of the tube. The region of interest is $0 \le r^* \le r_0(z^*)$, $0 \le z^* \le L^*$ (L^* being the finite length of the tube). Blood in physiological conditions may be considered as incompressible (Fung [4]). The assumption of Newtonian behaviour of blood is acceptable for high shear rate flow, e.g. in case of flow through large arteries (Pedley [9]). So the incompressible two-dimensional Navier-Stokes equations can be taken for the modelling of Newtonian fluid flow past smooth expansion. Let u^* and v^* be the axial and radial velocity components respectively, p^* the fluid pressure, ρ the constant density and ν denotes the kinematic viscosity of the fluid. Let U be the maximum inflow velocity specified in the inlet section or test section of the tube. We introduce the non-dimensional variables $t = t^*U/D_0, r = r^*/D_0, z = z^*/D_0, r_0(z) = r_0^*(z^*/D_0)/D_0, u = u^*/U, v = v^*/U, p = p^*/\rho U^2$ where D_0 is the diameter of tube in the unexpanded portion. The governing equations for incompressible fluid flow representing conservation of mass and momentum fluxes may be expressed in dimensionless variables as

$$r\frac{\partial u}{\partial z} + \frac{\partial vr}{\partial r} = 0, \tag{1}$$

$$\frac{\partial u}{\partial t} + \frac{\partial uv}{\partial r} + \frac{\partial u^2}{\partial z} + \frac{uv}{r} = -\frac{\partial p}{\partial z} + \frac{1}{Re}\left[\frac{\partial^2 u}{\partial r^2} + \frac{1}{r}\frac{\partial u}{\partial r} + \frac{\partial^2 u}{\partial z^2}\right], \tag{2}$$

$$\frac{\partial v}{\partial t} + \frac{\partial v^2}{\partial r} + \frac{\partial uv}{\partial z} + \frac{v^2}{r} = -\frac{\partial p}{\partial r} + \frac{1}{Re}\left[\frac{\partial^2 v}{\partial r^2} + \frac{1}{r}\frac{\partial v}{\partial r} + \frac{\partial^2 v}{\partial z^2} - \frac{v}{r^2}\right], \tag{3}$$

where $Re = U D_0/\nu$ is the Reynolds number.

2.1 Boundary conditions

The boundary conditions on the symmetry line of the tube are

$$\frac{\partial u}{\partial r} = 0, \qquad v = 0. \tag{4}$$

The no-slip boundary conditions are imposed at the solid wall as

$$u = v = 0 \quad \text{at } r = r_0(z). \tag{5}$$

The flow is considered to be fully developed at the inlet test section of the tube where the inlet section is considered at the position $z = -8$. The boundary conditions at the inlet section are

$$u = 2(1 - r^2), \qquad v = 0. \tag{6}$$

The downstream length (see Fig. 1) is sufficiently long so that the reattachment length is independent of the length of the calculation domain. The zero velocity gradient boundary conditions are used at the outlet cross-section of the tube

$$\frac{\partial u}{\partial z} = 0, \qquad \frac{\partial v}{\partial z} = 0. \tag{7}$$

2.2 Initial condition

The initial condition is that there is no flow inside the region of the tube except the parabolic velocity profile at the inlet. The flow is gradually developing as time elapses.

2.3 Transformation of basic equations

We consider a co-ordinate stretching in the radial direction which transforms the expanded tube into a straight circular tube is defined by

$$R = \frac{r}{r_0(z)}. \tag{8}$$

The function $r_0(z)$ is defined as (Pedrizzetti [10])

$$r_0(z) = 1 + \frac{d}{2}\left(1 + \tanh\frac{z}{d}\right) \tag{9}$$

where $r_0(z)$ denotes the radius of the tube in the expanded region. Here d is the value of expansion or the height of expansion. A schematic diagram of the expanded tube geometry considered in this analysis is given in Fig. 1 along with all relevant quantities. The tube under consideration is taken to be of finite length 50 for low Reynolds number flow. But suitable length is taken for the case of high Reynolds numbers so that the reattachment length is independent of this downstream distance.

3 Finite-difference formulation

A time marching procedure is adopted for the approximate solution of unsteady Navier-Stokes equations. Finite-difference discretization of the transformed governing equations with appropriate boundary conditions have been carried over in the present work in staggered grid, popularly known as MAC cell (Harlow and Welch [6]). In this type of grid alignment, the velocities and the pressure are evaluated at different locations of the control volume (rectangular cell as shown in Fig. 2). The use of the staggered grid permits coupling of the velocities u, v and the pressure p solutions at adjacent grid points. The time derivative terms are differenced according to the first order accurate two-level forward time differencing formula. The convective terms in the momentum equations are differenced with a hybrid second-order scheme consisting of central and upwinding differencing schemes. The diffusive terms are differenced using the three point central difference formula. The source terms are

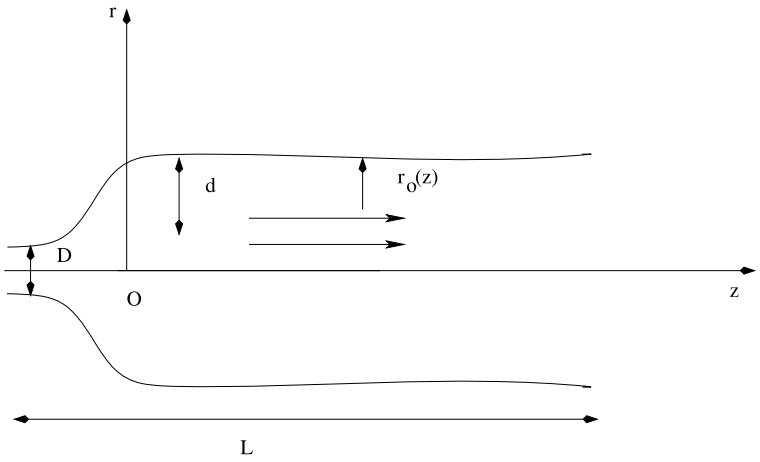

Fig. 1 Geometry of the tube with a smooth expansion

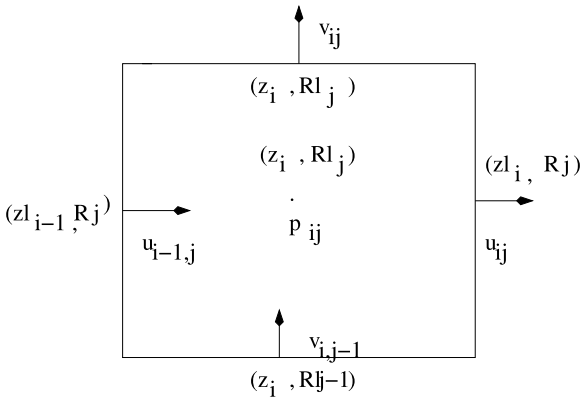

Fig. 2 Arrangement of dependent variables in a typical MAC cell

centrally differenced keeping the position of the respective fluxes at the centers of the control volumes. Thus, in finite-difference form with $t = n\delta t$, $z = i\delta z$, $R = j\delta R$ and $p(z, R, t) = p(i\delta z, j\delta R, n\delta t) = p^n_{i,j}$, superscript n refers to the time direction, δt is the time increment and $\delta z, \delta R$ are the length and width of the cell. The pressure derivatives are represented by forward difference formulae. Discretization of the continuity equation at (i, j) cell delivers

$$R_j r_0(z_i)\frac{u^n_{i,j} - u^n_{i-1,j}}{\delta z} - R_j^2 \frac{\partial r_0(z_i)}{\partial z}\frac{utc - ubc}{\delta R} + \frac{Rl_j v^n_{i,j} - Rl_{j-1} v^n_{i,j-1}}{\delta R} = 0 \quad (10)$$

where utc, ubc are defined as follows:

$$utc = 0.25(u^n_{i,j} + u^n_{i-1,j} + u^n_{i-1,j+1} + u^n_{i,j+1}),$$
$$ubc = 0.25(u^n_{i,j} + u^n_{i-1,j} + u^n_{i,j-1} + u^n_{i-1,j-1}).$$

Here $r_0(z_i)$ is calculated at $z = z_i$, $\frac{\partial r_0(z_i)}{\partial z}$ denotes the derivative of $r_0(z)$ with respect to z and calculated at $z = z_i$. The quantities (z_i, R_j), (zl_i, Rl_j) are the co-ordinates of the cell centre and the right top corner of the cell respectively. Considering the source, convective and diffusive terms at the n-th time level, the momentum equation in z-direction in finite difference form may be put as

$$\frac{u_{i,j}^{(n+1)} - u_{i,j}^{n}}{\delta t} = \frac{p_{i,j}^{n} - p_{i+1,j}^{n}}{\delta z} + \frac{R_j}{r_0(zl_i)} \frac{\partial r_0(zl_i)}{\partial z} \frac{p_t - p_b}{\delta R} + Ucd_{i,j}^{n} \tag{11}$$

where the terms p_t, p_b and $Ucd_{i,j}^{n}$ are defined as follows:

$$p_t = 0.25(p_{i,j}^{n} + p_{i+1,j}^{n} + p_{i,j+1}^{n} + p_{i+1,j+1}^{n}), \tag{12}$$

$$p_b = 0.25(p_{i,j}^{n} + p_{i+1,j}^{n} + p_{i,j-1}^{n} + p_{i+1,j-1}^{n}), \tag{13}$$

$$Ucd_{i,j}^{n} = \frac{1}{Re} Diff u_{i,j}^{n} - Conu_{i,j}^{n}. \tag{14}$$

p_t, p_b stand for pressure at the top and bottom middle positions of the u-momentum equation at n-th time level at (i, j)-th cell. The diffusive terms are discretized centrally. The finite difference equation approximating the momentum equation in the R-direction is

$$\frac{v_{i,j}^{(n+1)} - v_{i,j}^{n}}{\delta t} = \frac{1}{r_0(z)} \frac{p_{i,j}^{n} - p_{i,j+1}^{n}}{\delta R} + Vcd_{i,j}^{n} \tag{15}$$

where $Vcd_{i,j}^{n} = \frac{1}{Re} Diff v_{i,j}^{n} - Conv_{i,j}^{n}$.

Here $Vcd_{i,j}^{n}$ is the discretization of convective and diffusive terms of v-momentum equation at the n-th time level at cell (i, j). The diffusive and the convective terms in the v-momentum equation are differenced similar to that in u-momentum for the convective flux. The Poisson equation for pressure is obtained by combining the discretized form of the momentum and continuity equations. The final form of the Poisson equation for pressure is

$$\begin{aligned}
&(A + B + C + D)p_{i,j}^{n} - Ap_{i+1,j}^{n} - Bp_{i-1,j}^{n} + A_1 p_{i+1,j+1}^{n} - A_1 p_{i+1,j-1}^{n} \\
&\quad - A_2 p_{i-1,j+1}^{n} + A_2 p_{i-1,j-1}^{n} - (C - A_1 + A_2)p_{i,j+1}^{n} - (D + A_1 - A_2)p_{i,j-1}^{n} \\
&= -\left[\frac{Div_{i,j}^{n}}{\delta t} + R_j r_0(z_i) \frac{Ucd_{i,j}^{n} - Ucd_{i-1,j}^{n}}{\delta z} + \frac{Rl_j Vcd_{i,j}^{n} - Rl_{j-1} Vcd_{i,j-1}^{n}}{\delta R} \right]
\end{aligned} \tag{16}$$

where

$$A = \frac{r_0(z_i) R_j}{\delta z^2} = B, \tag{17}$$

$$C = \frac{Rl_j}{r_0(z_i)\delta R^2}, \tag{18}$$

$$D = \frac{Rl_{j-1}}{r_0(z_i)\delta R^2}, \tag{19}$$

$$A_1 = \frac{R_j^2 r_0(z_i)}{4r_0(zl_i)\delta z \delta R} \frac{\partial r_0(zl_i)}{\partial z}, \tag{20}$$

$$A_2 = \frac{R_j^2 r_0(z_i)}{4r_0(zl_{i-1})\delta z \delta R} \frac{\partial r_0(zl_{i-1})}{\partial z}. \tag{21}$$

Here $Div_{i,j}^n$ is the finite-difference representation of the divergence of the velocity field at cell (i, j). The pressure boundary condition is not needed for a MAC cell at the boundaries where the normal velocities are specified. However, the pressure boundary conditions at the nonsolid and at the outer cell have to be specified. Neumann type boundary conditions have been specified here and evaluated from the unsteady momentum equations (Roache [11]).

Equation (16) is solved iteratively, by the SOR (successive over-relaxation) method by exploiting appropriate boundary conditions. After performing a few iteration steps with the pressure equation, the pressure-velocity corrections are invoked. The method is continued until it achieves a satisfactory level of divergence value (in this case, we fixed the divergence values at 0.00001). The same procedure is followed for the derivation of pressure-velocity corrections.

3.1 Stability criteria of the scheme

The time step is governed by the following two restrictions. The first restriction is related to the convection of the fluid. So the time step must satisfy

$$\delta t_1 \leq \text{Min}\left[\frac{\delta z}{|u|}, \frac{\delta R}{|v|}\right]_{ij}, \tag{22}$$

where minimum is taken in the global sense. Secondly, momentum must not diffuse more than one cell in one time step. This condition, which is related to the viscous effects, according to Hirt's [7] stability analysis implies

$$\delta t_2 \leq \text{Min}\left[\frac{Re}{2} \frac{\delta z^2 \delta R^2}{(\delta z^2 + \delta R^2)}\right]_{ij}. \tag{23}$$

Hence, in our computations we take

$$\delta t = c\text{Min}\left[\delta t_1, \delta t_2\right], \tag{24}$$

where c is a constant lying between 0.2 to 0.4. A typical value of δt is 0.005 for $\delta z = 0.05$ and $\delta R = 0.05$ for the Reynolds number smaller than 1300. And the upwinding parameter β used in the convective terms differencing is selected according to the inequality

$$1 \geq \beta \geq \text{Max}\left[\left|\frac{u\delta t}{\delta z}\right|, \left|\frac{v\delta t}{\delta R}\right|\right]_{ij}. \tag{25}$$

The accuracy in time is of $O(\Delta t)$.

Table 1 Results of different grid sizes for a smooth expanded tube at $Re = 10$, $d = 0.25$

Grid	Property	$R \to 0.25$	0.50	0.75	1.0
1200×40	ψ	0.02152	0.08055	0.16105	0.23700
600×20	ψ	0.02161	0.08074	0.16123	0.23708
1200×40	ω	0.23547	0.45382	0.66902	0.88687
600×20	ω	0.24311	0.45874	0.67045	0.88472

Table 2 Results of different grid sizes for a smooth expanded tube at $Re = 1200$, $d = 0.25$

Grid	Property	$R \to 0.25$	0.50	0.75	1.0
1200×40	ψ	0.02699	0.09861	0.18941	0.26950
600×20	ψ	0.02708	0.09875	0.18950	0.26957
1200×40	ω	0.40423	0.75408	0.87344	0.88325
600×20	ω	0.40737	0.75923	0.87924	0.88872

4 Results and discussions

The present study considers flow in a tube with expansion. An uniform grid distribution of size 0.05 is taken in both directions of the tube. The downstream length of the expanded tube was taken sufficiently long to permit the flow to redevelop into a fully developed flow i.e., the condition $\frac{\partial u}{\partial z} = 0$ is properly satisfied. With increasing Reynolds number and also with the increasing height of expansion of the tube, the length of flow development downstream of the expansion increased. In the present numerical simulation, a sufficient downstream length is set so that the reattachment length is unaltered and tested for each of the Reynolds number studied. The present numerical scheme is stable for higher Reynolds number flows.

After obtaining the desired level of convergence the calculations for ψ and ω are performed with the help of the formulae $u = \frac{1}{r}\frac{\partial \psi}{\partial r}$, $v = -\frac{1}{r}\frac{\partial \psi}{\partial z}$ and $\omega = (\frac{\partial v}{\partial z} - \frac{\partial u}{\partial r})$. Using the two-stage numerical algorithm, we compute the stream function (ψ) and vorticity (ω) in an expanded tube for different values of R at $Re = 10$ and $d = 0.25$ for different grid distributions and it is given in Table 1 for $z = 6.2$.

This shows that the results for the grid size 600×20 is reasonably good. The actual computation for the expanded case have been carried out on a grid 1200×40, while for higher Reynolds number a grid size of 2000×40 has been chosen. The grid independence test is also performed for $Re = 1200$ for different values of R and for $d = 0.25$ and it is given in Table 2 for fixed value of z ($z = 18.2$).

We now give our attention for analyzing flow features in the region of expansion and the corresponding relations to the arterial diseases. Wall pressure plays an important role in case of fluctuations of the flow variables in the vicinity of the complex flow region. The non-dimensional pressure distribution along the wall of the tube in the axial direction for expanded tube at $Re = 1200$ with expansion height $d = 0.25$ is plotted in Fig. 3. The curve shows a rapid fall in pressure as the expansion is approached and recovers slightly after it. The fluctuations of wall pressure are key

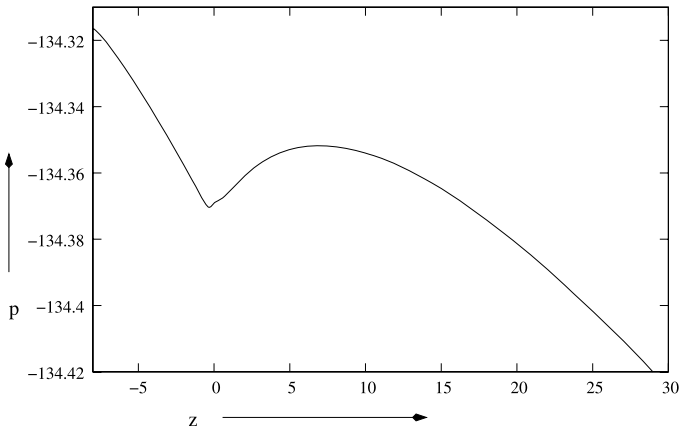

Fig. 3 Pressure distribution at $Re = 1200$ for $d = 0.25$

ingredients in acoustical techniques for detecting arterial disease (Ask et. al. [1]). The variable wall pressure can damage and weaken the internal wall (intima) of the artery.

The velocity profiles are of some interest since they provide a detailed description of the flow field. Fig. 4a exhibits the variation of center line velocity in axial direction for different Reynolds numbers and for the expansion height $d = 0.25$. Due to formation of recirculation zone near the wall, the maximum centre line velocity occurs slightly in the downstream of the expansion. From Fig. 4b it is very clear that a larger distance is required for the centre line velocity to recover its initial value. The figure also exhibits that the zero gradient velocity boundary conditions are satisfied at the outlet. The comparison of centre line velocity distribution at $Re = 1200$ for different expansion height has been given in Fig. 5.

The velocity profiles are plotted in Fig. 6 for several axial positions at $Re = 1200$ for the expansion height $d = 0.5$. The region of reversal flow is evidenced in this figure. In this region, the components of velocity undergo a change in sign.

The development of shear stress at the wall is of particular relevance for the localization and prediction of arterial diseases.

The stress on the wall denoted by $\tau_w[= \mu(\frac{\partial v}{\partial z} + \frac{1}{r_0(z)}\frac{\partial u}{\partial R})_{R=1}]$ of the artery plays an important role in arterial disease. With unsteady flow in arterial curvature and bifurcation sites, regions are present in which the flow is reversed during part of the cardiac cycle. So the wall shear stress varies from a large magnitude in one direction to negative values during part of the cycle.

In Fig. 7, the distribution of wall shear stresses (τ_w) for the Reynolds numbers $Re = 200, 400, 800, 1200$ in the tube are shown for the expansion height $d = 0.25$. The largest magnitude of the wall stress or skin friction is found near the end of the expansion which is consistent with the high streamwise velocity at this location. It is very interesting to note that, the peak value of τ_w decreases with increasing Reynolds numbers while at a particular axial position (between the cross-over points), the wall shear stress increases with the increasing Reynolds numbers. The peaks of the shear

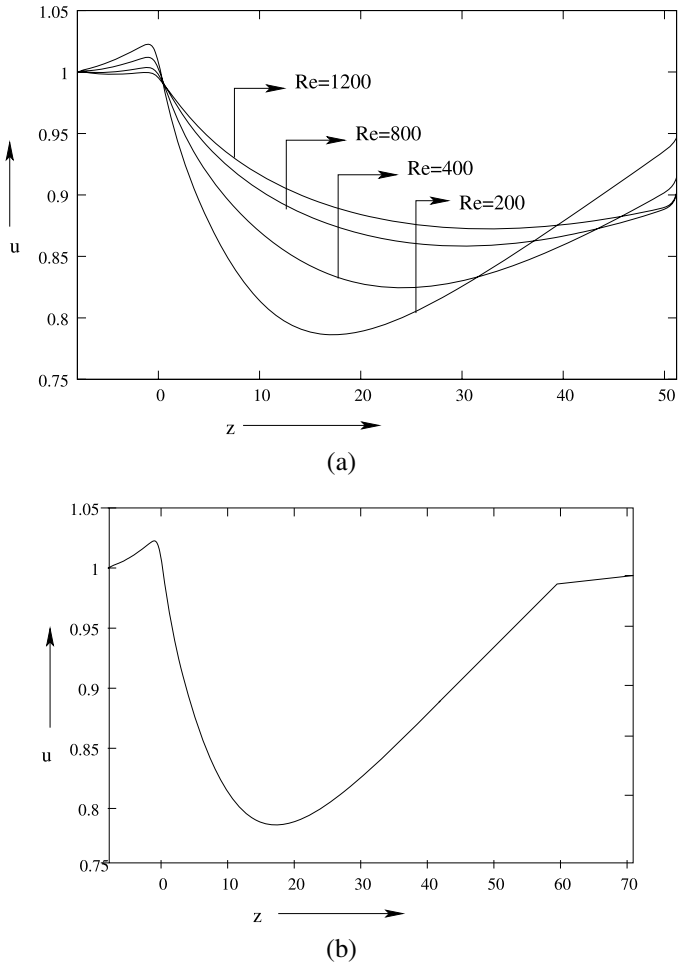

Fig. 4 (**a**) Centreline velocity distribution for $d = 0.25$ at different Reynolds numbers. (**b**) Centreline velocity distribution for $d = 0.25$ at $Re = 200$

stresses are believed to cause severe damage to the arterial lumen which in turn help in detecting the aggregation sites of platelets (Fry [3]). The negative values of the wall shear stresses indicate the separating region. Separation of the boundary layer gives rise to the flow structure which has important implications in understanding and predicting the flow characteristics. Negative shear is substantially more prevalent than positive because of separation.

The effects of increasing height of expansion (increasing d) on the wall shear stress distribution at $Re = 1200$ is very clear from Fig. 8. It is evident from this figure that the peak value of τ_w decreases with the increasing height. Also at a particular axial position, the wall shear stress decreases with the increasing height of expansion.

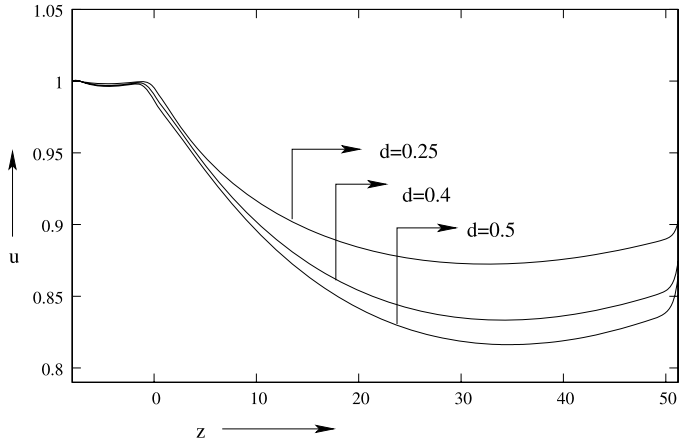

Fig. 5 Centreline velocity distribution at $Re = 1200$ for different d

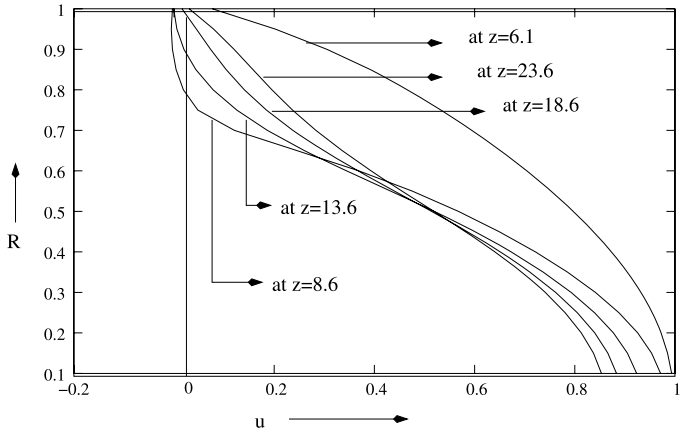

Fig. 6 Velocity profiles for several axial positions z where z is the distance from the inlet test section at $Re = 1200$ for $d = 0.5$

5 Conclusions

The axi-symmetric steady flow of a viscous Newtonian incompressible fluid through a tube with a smooth expansion has been simulated numerically with a view to understanding the fluid dynamical phenomena corresponding to post-surgical carotid conditions. A stable two-stage numerical algorithm is used for this axi-symmetric flow. Flow feature depends on the expansion height and also on the Reynolds number as follows:

(i) As the expansion is approached, a rapid fall in pressure is noticed.
(ii) Centreline velocity increases with increasing Reynolds number but decreases with increasing height of expansion.

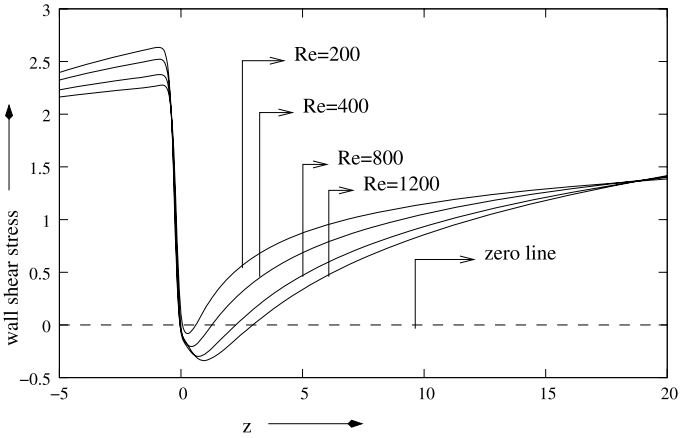

Fig. 7 Wall shear stress distribution at different Reynolds numbers for $d = 0.25$

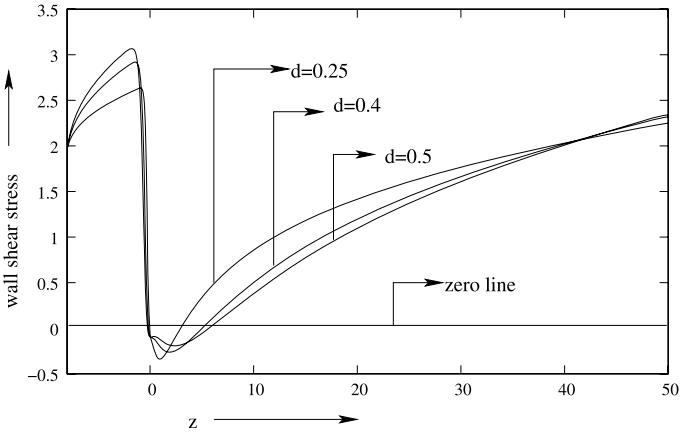

Fig. 8 Wall shear stress distribution for different d at $Re = 1200$

(iii) Length of flow separation is noticed to increase with increasing Reynolds number as well as with the increasing height of expansion.
(iv) The peak value of wall shear stress decreases with increasing Reynolds number and also with the increasing height of expansion.

The main contribution of the present paper is to estimate accurately the wall shear stress, flow rate and the length of separation for slowly varying tube expansion.

Acknowledgement The authors are thankful to the honourable reviewers for constructive suggestions. One of the author (G.C. Layek) acknowledges the financial support from CSIR, India for carrying out this work.

References

1. Ask, P., Hok, B., Lyod, D., Terio, H.: Bio-acoustic signals from stenotic tube flow: state of the art and perspectives for future methodological development. Med. Biol. Eng. Comput. **33**, 669–675 (1995)
2. Formaggia, J.F., Gerbean, F.N., Quarteroni, A.: On the coupling of 3D and 1D NS equations for flow problems in complaint vessels. Comput. Methods Appl. Mech. Eng. **191**, 561–582 (2001)
3. Fry, D.L.: Certain histological and chemical responses of the vascular interface of acutely induced mechanical stress in the aorta of the dog. J. Circ. Res. **24**, 93–109 (1969)
4. Fung, Y.C.: Biomechanics, Mechanical Properties of Living Tissues. Springer, New York (1981)
5. Hammad, K.J., Otugen, M.V., Vradis, G.C., Arik, E.B.: Laminar flow of a nonlinear viscoplastic fluid through an axisymmetric sudden expansion. Trans. ASME **121**, 488–495 (1999)
6. Harlow, F.H., Welch, J.E.: Numerical calculation of time dependent viscous incompressible flow of fluid with free surface. Phys. Fluids **8**, 2182–2189 (1965)
7. Hirt, C.W.: Heuristic stability analysis of finite difference equations. J. Comput. Phys. **2**, 339–355 (1968)
8. Ling, S.C., Atabek, H.B.: A nonlinear analysis of pulsatile flow in arteries. J. Fluid Mech. **55**, 493–511 (1972)
9. Pedley, T.J.: The Fluid Mechanics of Large Blood Vessels. Cambridge University Press, Cambridge (1980)
10. Pedrizzetti, G.: Unsteady tube flow over an expansion. J. Fluid Mech. **310**, 89–111 (1996)
11. Roach, M.R.: Change in arterial distensibility as a cause of poststenotic dilatation. Am. J. Cardiol. **12**, 802–815 (1963)
12. Taylor, C.A., Hughes, T.J.R., Zarins, C.K.: Finite element modelling of blood flow in arteries. Comput. Methods Appl. Mech. Eng. **158**, 155–196 (1998)
13. Yamaguchi, T.: Computational mechanical model studies in the cardiovascular system. In: Yamaguchi, T. (ed.) Clinical Application of Computational Mechanics to the Cardio Vascular System, pp. 3–19. Springer, Berlin (2000)

G.C. Layek was born in Bankura District, West Bengal. He obtained the B.Sc. Honours degree in Mathematics from the University of Burdwan, Burdwan. Then he obtained M.Sc. and Ph.D. degrees from I.I.T., Kharagpur in 1990 and 1996 respectively. He carried out his post-doctoral research work in I.S.I., Kolkata and was a visiting scientist of I.S.I., Kolkata till 2000. He joined the Department of Mathematics, The University of Burdwan as a Lecturer in 2000 and now he is in the post of Reader in the same Department. His research interest includes the flow separation, pulsatile flow, turbulent, boundary layer flows including heat and mass transfer and Dynamical systems.

S. Mukhopadhyay was born and brought up in Burdwan, West Bengal. She obtained the B.Sc. Honours and M.Sc. degrees in Mathematics from the University of Burdwan. She joined as a regular research scholar in the Department of Mathematics, the University of Burdwan in 2002 and was awarded her Ph.D. degree in Fluid Mechanics from the same University in 2007. She joined as a Lecturer in Mathematics in M.U.C. Women's College, Burdwan in 2006. Her research interest covers the areas of the application of flow separation, particularly, in bio-fluid dynamics and analysis of boundary layer flows including the heat and mass transfer.